*Int. J. Electrochem. Sci.*, 16 **(2021)** Article ID: 21089, doi: 10.20964/2021.08.06

International Journal of
ELECTROCHEMICAL
SCIENCE
www.electrochemsci.org

# Investigation of Electrochemical Behavior of *4-(2-Pyridylazo)resorcinol* and its $Cu^{2+}$ Complex by Using Polarographic and Voltammetric Techniques

*Yeliz KARAMAN*[1] *and Necati MENEK*[2]

[1] Sinop University, Sciences and Arts Faculty, Department of Chemistry, 57000, Sinop, Turkey
[2] Ondokuz Mayıs University, Sciences and Arts Faculty, Department of Chemistry, 55139, Kurupelit-Samsun, Turkey
*E-mail: nmenek@omu.edu.tr, ykaraman@sinop.edu.tr

*Received:* 30 March 2021 / *Accepted:* 18 May 2021 / *Published:* 30 June 2021

In this work, the electrochemical behavior of 4-(2-pyridylazo)resorcinol (PAR) azo dye was studied in Britton-Robinson (BR) buffer (pH 2.0-12.0) media by employing square wave voltammetry (SWV), differential pulse polarography (DPP), direct current polarography (DCP) and cyclic voltammetry (CV) techniques. From the polarographic and voltammetric results, the electrochemical reaction mechanism of the azo dye has been proposed. At the same time, the electrochemical behavior of the copper(II) complex with PAR was investigated by using SWV in 0.1 M $KNO_3$ supporting electrolyte. SWV behavior of Cu(II)-PAR complex at different metal and ligand concentrations have been determined in $KNO_3$ supporting electrolyte media. The metal:ligand molar ratio and stability constant of the Cu(II)-PAR complex were determined to be 1:2 and $5.42x10^{10}$, respectively.

**Keywords:** Azo dye, reduction, reaction mechanism, metal complex.

## 1. INTRODUCTION

Heterocyclic azo dyes are commonly employed as complexometric agents for spectrophotometric detection of numerous elements [1-3]. To date, many workers have used polarographic and voltammetric methods to develop improved sensitive techniques for detecting metal ions with heterocyclic azo dyes as complexing indicators [4-14].

Azo dyestuffs are always considered worth researching due to their scientific studies, since they have carcinogenic properties and have a wide application area in the paint and textile industry. In the textile industry, the creation of colors in different characteristics is usually achieved with the help of the complexes from which the dyestuffs are formed. Therefore, it is necessary to define the properties of the complexes formed by the relevant azo dyestuffs. At the same time, metals are selectively determined

with the help of the complexes they form. Due to these properties, suitable solution mediums are preferred for analytical adaptations so that they are least affected by matrix effects [6, 11].

Azo dyestuffs form stable complexes with many metals. Dyestuffs increase selectivity in analytic applications, especially in the analysis of metal ions. Extractants suited to this class contain 1-(2-pyridylazo)-2-naphthol (PAN), PAR, 4-(2-thiazolylazo)resorcinol (TAR) and similar group dyes. PAN, PAR, and TAR produce complexes with numerous metal ions containing copper, cadmium, zinc etc., though the pH has a deep influence on the complexation process [15].

PAR is one of the derivative of 2-pyridylazo used as chromogenic chelator for the quantitative analysis of different metal ions in trace amounts. The metal:ligand ratios of complexes of copper(II) with PAR in different media have been found to be 1:1 and 1:2 by spectrophotometric methods. The logarithm stability constants of the $Cu(PAR)_2$ complex were found to be as 12.31 and 11.83 for molar ratio and continuous variation methods, respectively [16].

Heterocyclic azo dyes are of great interest because they are sensitive and selective chromogenic reagents. To determine the sensitivity and selectivity of these compounds and their metal complexes, the electrochemical behavior of the dyes and their metal complexes have been investigated [4-14].

The goal of the study is to investigate the electrochemical reaction mechanism of PAR and determine the metal:ligand ratio and stability constant of the copper(II)-PAR complex by using polarographic and voltammetric techniques.

## 2. EXPERIMENTAL

4-(2-Pyridylazo)resorcinol monosodium salt hydrate was bought from Sigma-Aldrich and employed without pretreatment. A $10^{-3}$ M stock solution of PAR was prepared in ultrapure water. A 0.04 M BR buffer solution has been prepared by mixing 0.04 M $H_3PO_4$, 0.04 M $CH_3COOH$ and 0.04 M $H_3BO_3$. Concentrated sodium hydroxide solution was employed for desired pH adjustment. All chemicals used were of p.a. purity.

The electrochemical studies were performed with a Metrohm 757 VA Computrace Electrochemical Analyzer in BR buffer (pH 2.0-12.0) solutions at room temperature. The three electrode system was composed of multimode electrode (dropping mercury electrode (DME), static mercury drop electrode (SMDE) and hanging mercury drop electrode (HMDE)), a Ag/AgCl reference electrode and a Pt wire auxiliary electrode. The electrochemical experiments were conducted by employing SWV, DPP, DCP and CV methods. Before starting the electrochemical analysis, clean dry nitrogen gas was passed through the solutions for five minutes to remove the dissolved oxygen gas. The copper(II) nitrate hexahydrate ($Cu(NO_3)_2.6H_2O$) solution used in the experiments was prepared employing ultrapure water. The transition metal complex studies of the azo dye were performed in 0.1 M $KNO_3$ medium.

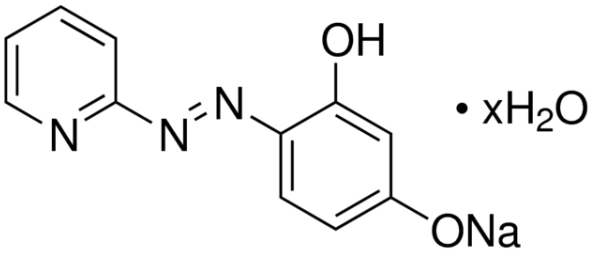


**Scheme 1.** Molecular structure of the 4-(2-pyridylazo)resorcinol monosodium salt hydrate.

## 3. RESULTS AND DISCUSSION

The polarographic and voltammetric behavior of PAR was examined by employing SWV, DPP, DCP and CV methods in BR (pH 2.0-12.0) buffer. Voltammograms and polarograms of PAR are presented in Fig. 1. As stated in Fig. 1, one cathodic peak was seen at all pH values. The peaks obtained from the SWV and DPP techniques correspond to the reduction of the azo group in BR buffer (Fig. 1). The variation of peak potentials ($E_p$) versus pH of PAR is presented in Fig. 2 for the SWV and DPP methods. The shift of the reduction peak potentials towards more negative values with increasing pH shows that hydrogen ions take part in the electrode reaction mechanism [17-23].

Linear variations in the reduction peak potentials of PAR versus pH are shown in Table 1 for the SWV and DPP methods. The linear variations in the peak potentials with pH can be given as $E_p(V) = 0.0125-0.0751pH$ and $E_p(V) = 0.2146-0.0853pH$ for the SWV and DPP methods, respectively, in BR buffer solutions.

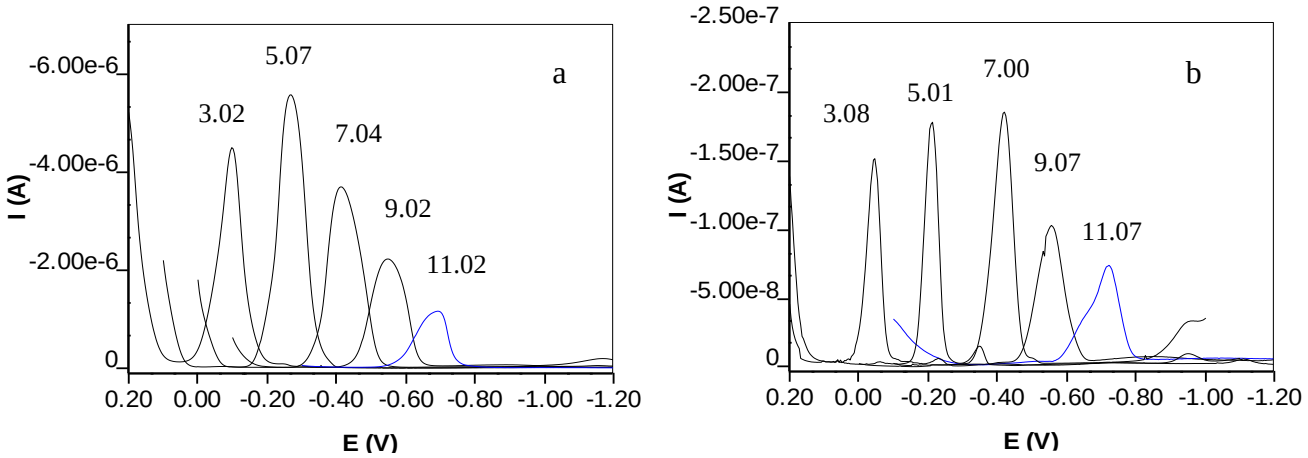


**Figure 1.** Voltammograms and polarograms of $9.90.10^{-6}$ M PAR in BR buffer (0.04 M) (a) SWV, pH 3.02, 5.07, 7.04, 9.02, and 11.02, scan rate ($v$) = 200 mV/s, (b) DPP, pH 3.08, 5.01, 7.00, 9.07, and 11.07, $v$ = 4 mV/s.

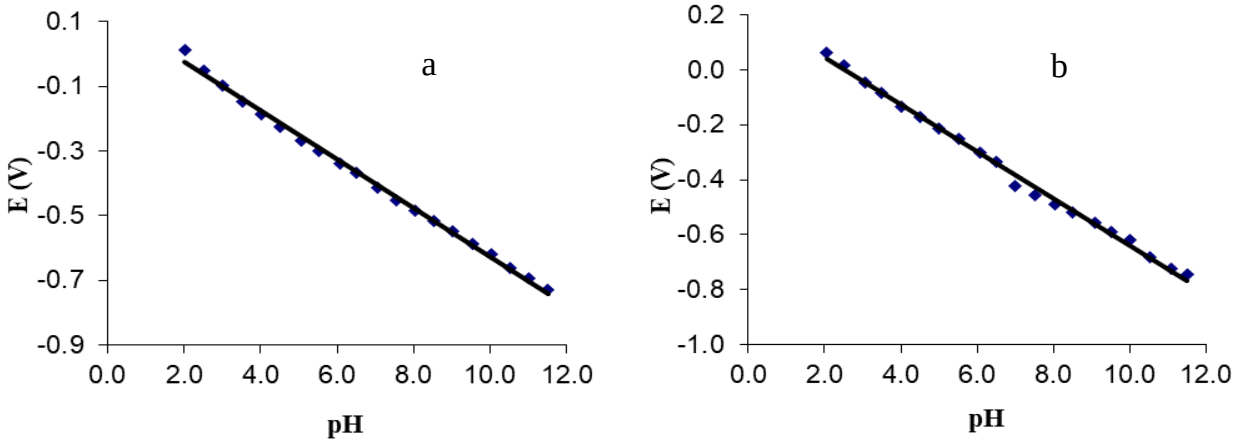


**Figure 2.** Dependence of the reduction peak potentials versus pH in BR buffer for 9.90x10$^{-6}$ M PAR a) SWV, $v$ = 200 mV/s b) DPP, $v$ = 4 mV/s, drop time 1 s.

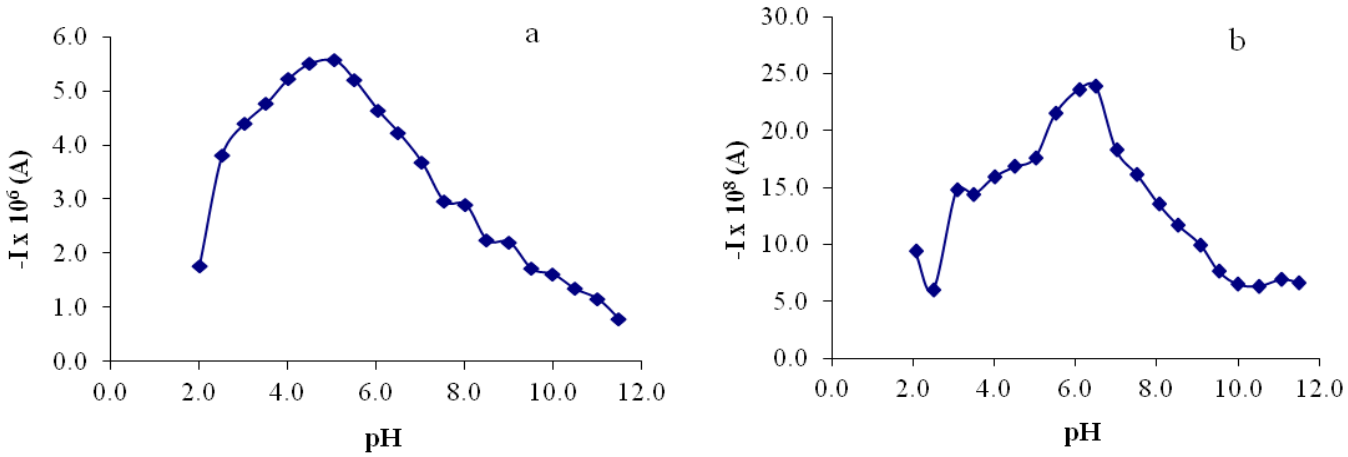


**Figure 3.** The variation in cathodic peak currents versus pH in BR buffer for 9.90x10$^{-6}$ M PAR a) SWV, $v$ = 200 mV/s b) DPP, $v$ = 4 mV/s.

As shown in Fig. 3, with SWV, the peak current of the dyestuff increases between pH 2.0 and 5.0 and a decrease is observed with increasing pH after pH 5.0. An increase is seen in the peak current of the dyestuff between pH 2.0 and 6.5 and a decrease is observed after pH 6.5 with the DPP technique. These results showed that the protonation of the nitrogen atom changes at pH 2.0–5.0 and 2.0-6.5 for two techniques.

**Table 1.** Dependence of peak potentials on pH.

| **Medium** | **pH** | **Peak equation** | **r$^2$ (Regression coefficient)** | **Method** |
|---|---|---|---|---|
| BR (0.04 M) | 2.0-12.0 | $E_p$ (V) = 0.0125-0.0751pH | 0.9970 | SWV |
| BR (0.04 M) | 2.0-12.0 | $E_p$ (V) = 0.1316-0.0821pH | 0.9882 | CV |
| BR (0.04 M) | 2.0-12.0 | $E_p$ (V) = 0.2146-0.0853pH | 0.9962 | DPP |

*3.1. DCP studies*

Fig. 4 demonstrates characteristic DC polarograms of the azo dye in BR buffer; one reduction wave is seen in the pH range of 2.0 to 12.0 with a scan rate of 4 mV/s. It follows from the dependence of the limiting current on the pH that twice as many electrons are replaced in the strongly alkaline region as in the acidic region.

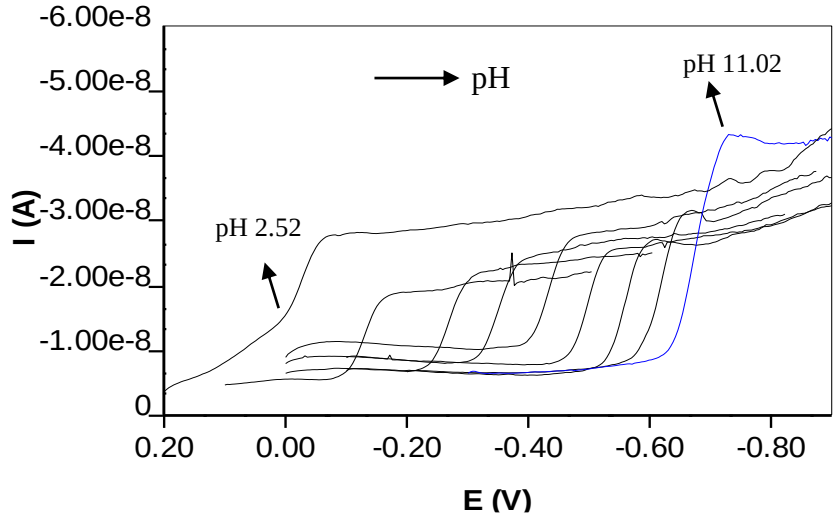


**Figure 4.** DC polarograms of 9.90x10$^{-6}$ M PAR in BR (0.04 M) buffer pH 2.52, 3.52, 5.07, 6.06, 7.04, 8.04, 9.02, 10.01 and 11.02 media, $v$ = 4 mV/s.

Logarithmic analyses were made from DCP data for cathodic waves in BR buffer (2.0–12.0). The Heyrovsky-Ilkovic equation was employed to calculate the αn values [24-26].

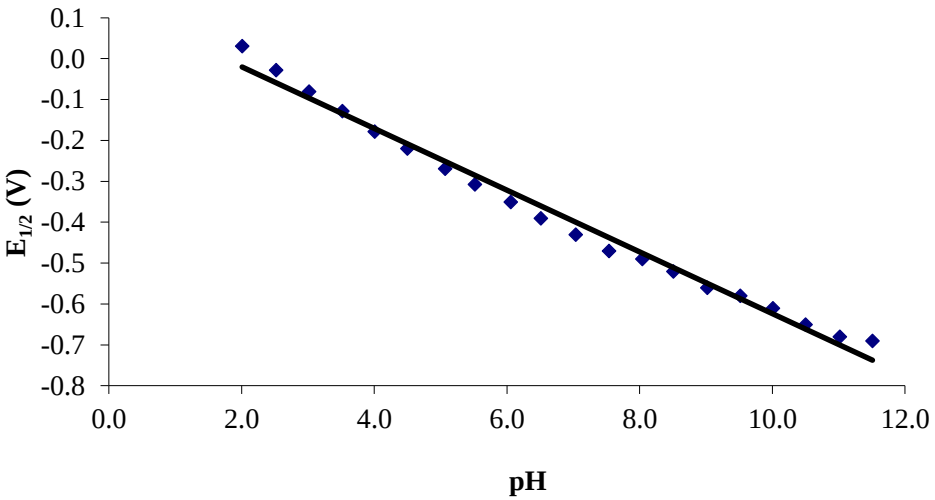


**Figure 5.** Plot of $E_{1/2}$ values versus pH in BR buffer, $v$ = 4 mV/s.

As seen in Fig. 4, the limiting current becomes approximately constant between the pH values of 2.0 and 10.5 and shows a gradual increase in strongly alkaline media (pH ≥ 11.0), twice its original value

in the pH range of 2.0 to 10.5. This behavior conforms to the reality that the electrode reaction of the azo dye proceeds with two and four electrons in acidic and strongly basic solutions, respectively. In strongly basic media, the azo dye undergoes a two-step reaction. In the first stage, the dye is reduced to a hydrazo and then, in the second stage, hydrazo form is reduced to aniline species. The peak potentials of the two stages are approximately equal. The reduction of PAR at the SMDE is altered depending on the pH. The $E_{1/2}$ potentials shift to higher values with an increase in the pH (Fig. 5).

Additionally, the $E_p$-pH graphs for the reduction wave of PAR are straight lines, with the slope (S) values given in Table 1. The number of protons and electrons taking part in the rate-determining reaction was determined by using the slopes obtained from the E versus log ($I/I_d$-I) and pH versus $E_{1/2}$ graphs, respectively (Figs. 5, 6). At pH 2.0-10.5 range, the αn values show that the electrode reaction involves two electrons, corresponding to a reduction of the azo dye to the hydrazo form, while a four-electron process proceeds in strongly alkaline media (pH ≥ 11.0), which corresponds to cleavage of the azo bridge. The results suggest that two protons and two electrons (pH 2.0-10.5) participate in the rate-limiting step of the reactants.

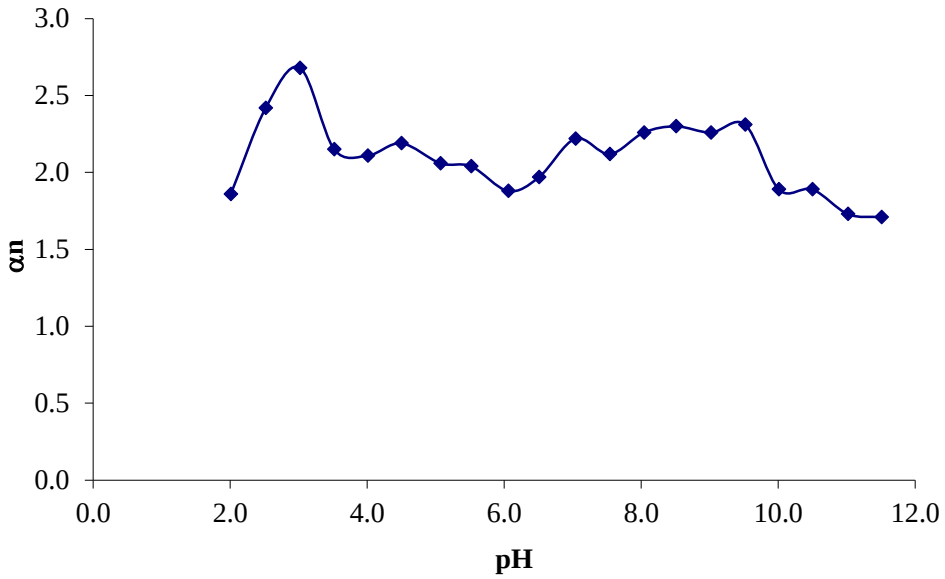


**Figure 6.** Plot of αn values versus pH for PAR in BR buffer.

*3.2. CV studies*

The CV technique is necessary to elucidate the electrochemical behavior of azo compounds [26]. Generally, pH is an important factor that usually affects the appearance of voltammograms, so it is significant to elucidate the impacts of pH on electrochemical processes. The CV voltammograms of the azo dye recorded in the range of pH 2.0-12.0 are presented in Fig. 7. Variations in cathodic peak potentials and peak currents versus pH are given in Fig. 8 for the CV technique. The linear variation of the peak potential with pH can be given as $E_p$ (V) = 0.1316-0.0821pH for the CV analysis in BR buffer (Table 1).

In strongly alkaline media (pH ≥ 11.0), the cathodic process is not reversible because no anodic peak was seen on the reverse scan. However, in the range of pH 2.0–10.5, a reversible electrode reaction was observed, as evidenced by the anodic peak present in the reverse scan.

The peak potential values shift to more negative values with each increasing pH, which confirmed the contributed of hydrogen ions in the cathodic electrode reactions as determined by means of SWV, DPP and DCP **(**Figs. 2, 5) [27-29].

The dependence of the scan rate ($v$) on the reduction peak current ($I_p$) of the azo dye at a HMDE was studied in BR buffer at various pH values (pH 4.52, 7.08, and 9.53). As seen from the equation $I_p = Av^x$, there is a linear relationship between the peak current and scan rate ($v$). x can take the values 1.0 and 0.5 for adsorption and diffusion-controlled reactions, respectively. For PAR, the regression of log($I_p$) versus log($v$) gave slope values of 1.11, 1.04 and 0.93 for pH 4.52, 7.08 and 9.53, respectively, indicating that the electrode reaction is adsorption-controlled [30].

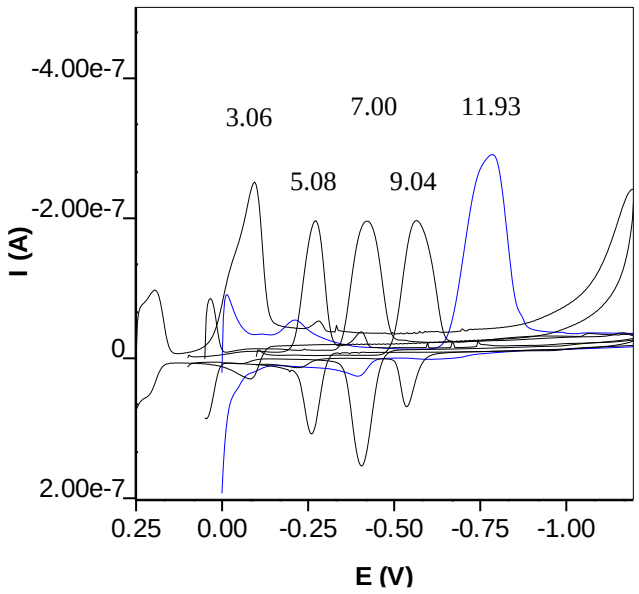


**Figure 7.** CV voltammograms of 9.90x10$^{-6}$ M PAR in BR (0.04 M) buffer (pH 3.06, 5.08, 7.00, 9.04, and 11.93) solutions, $v$ = 200 mV/s.

The peak potential changes to more negative values with increasing scan rate from 5 to 1000 mV/s, (Fig. 9) [31,32]. The $I_p$ versus $v^{1/2}$ relation is not linear, and the $I_p/v^{1/2}$ slope increases with increasing scan rate. This result confirms that the azo compound undergoes a complex electrochemical reaction on the electrode surface [33]. Such behavior is determinative of an EC mechanism, as demonstrated in previous studies [34-39].

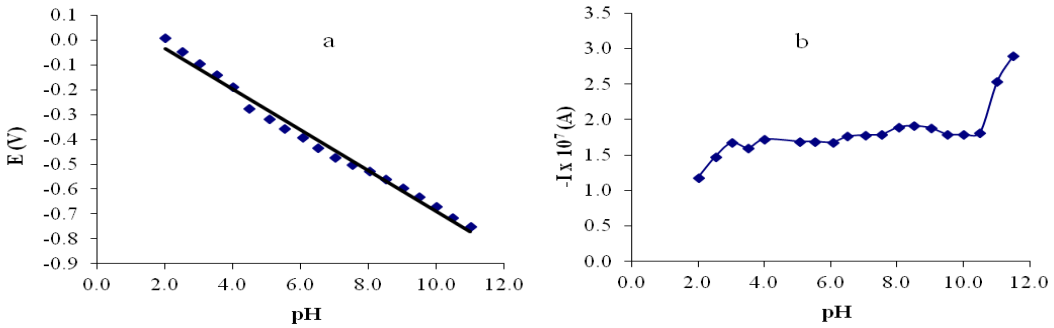


**Figure 8.** Plot of cyclic voltammetric a) reduction peak potentials and b) reduction peak currents versus pH in BR buffer for 9.90x10$^{-6}$ M PAR, $v$ = 200 mV/s.

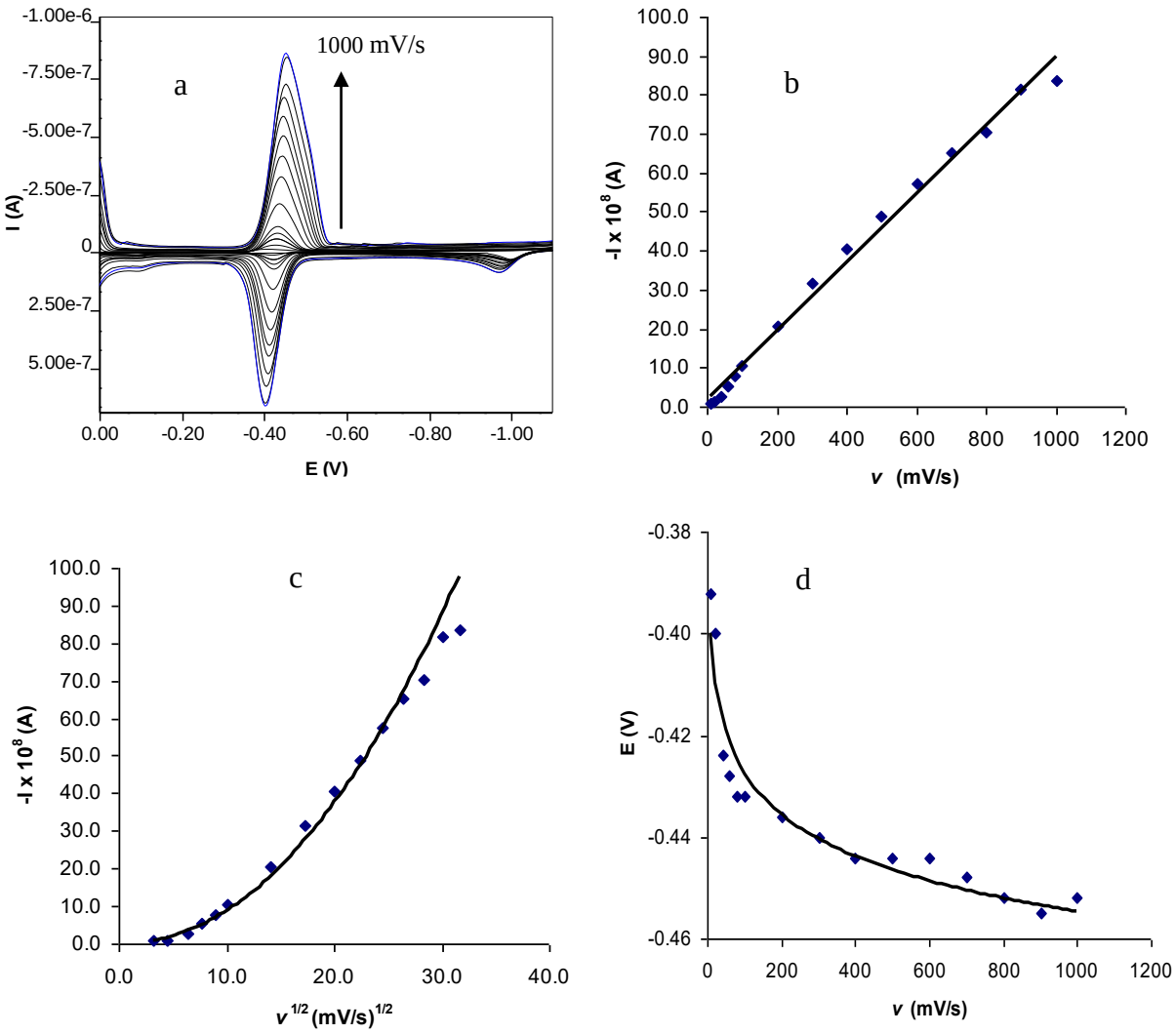


**Figure 9.** a) The variation in cyclic voltammograms of 9.90x10$^{-6}$ M PAR with scan rate at pH 7.08 in BR (0.04 M) buffer, b) The variation in cathodic peak currents with scan rate at pH 7.08, c) The variation in cathodic peak currents with square root of scan rate at pH 7.08, d) The variation in cathodic peak potentials with scan rate at pH 7.08, ($v$ = 5-1000 mV/s).

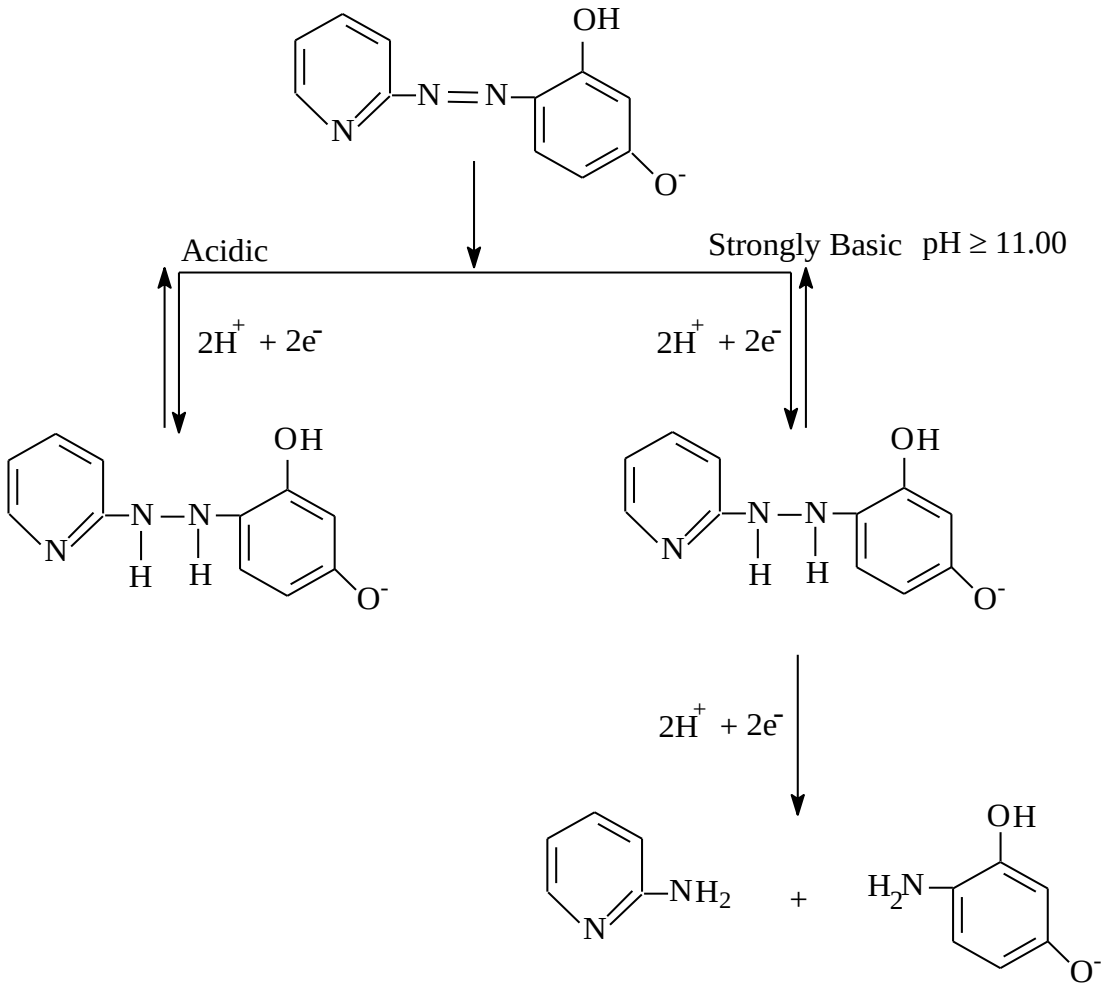


**Scheme 2.** Reaction mechanism of PAR.

*3.3. Copper Complex Studies*

Investigation of metal complexes is performed in different solution media. The aim is to increase the selectivity. Therefore, metal complexes may exhibit different characteristics depending on the solution medium. For this purpose, potassium nitrate medium was preferred to minimize the matrix effects of copper(II)-PAR complex.

To determine the metal:ligand ratio of the Cu(II)-PAR complex, SW voltammograms were recorded by adding the ligand solution to the metal and metal solution to the ligand in 0.1 M $KNO_3$ supporting electrolyte. It was observed that a pink complex was formed by adding the ligand to Cu(II) and Cu(II) to the ligand. Using the data obtained from the SW voltammograms, the current and potential values of the reduction peaks of the ligand and complex were plotted against increasing Cu(II) concentration.

First, 800 µl $10^{-4}$ M PAR solution was added to 10 ml 0.1 M $KNO_3$ solution in the voltammetric cell. Then, 100-3500 µl $10^{-4}$ M Cu(II) solution was added to 800 µl $10^{-4}$ M PAR solution, and SW voltammograms were recorded. SW voltammograms of PAR obtained in 0.1 M $KNO_3$ supporting

electrolyte are presented in Fig. 10. Examining the SW voltammograms in Fig. 10, two different reduction peaks are observed at potential values of -0.054 V and -0.613 V for the azo dye.

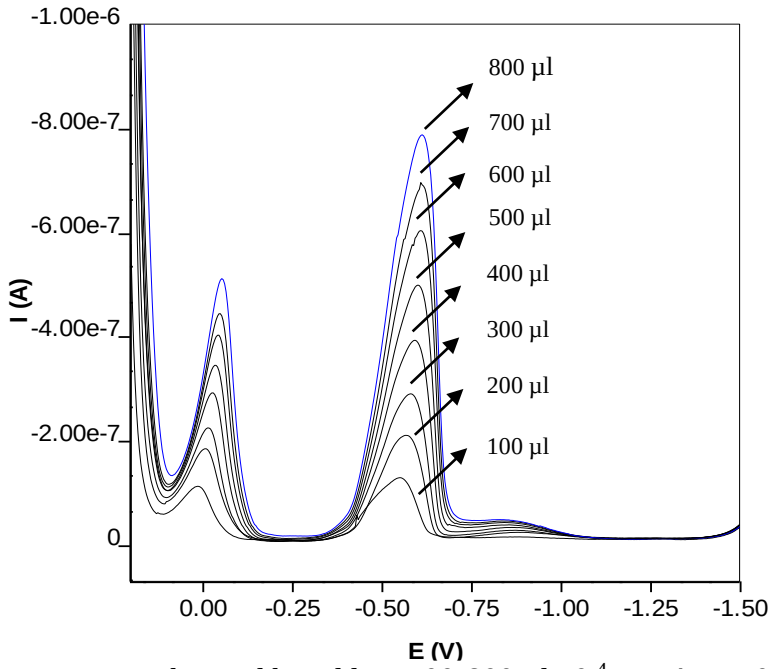


**Figure 10.** SW voltammograms obtained by adding 100-800 µl $10^{-4}$ M PAR in 0.1 M $KNO_3$ medium, *v* = 200 mV/s.

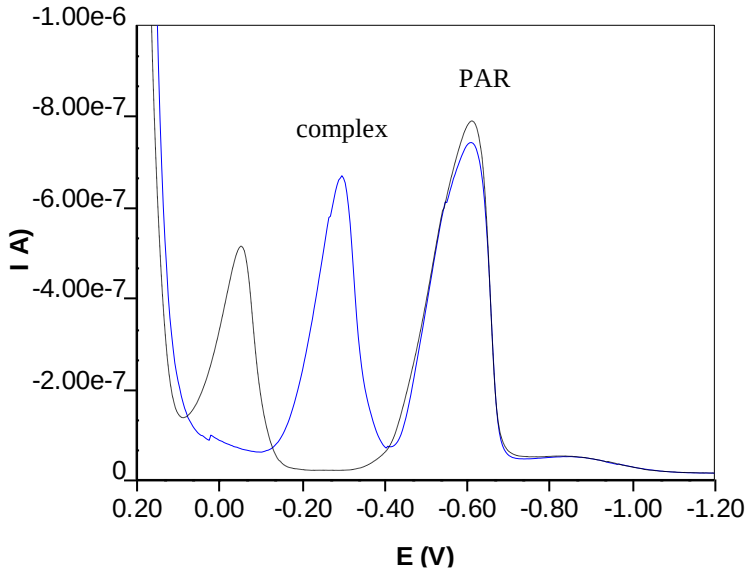


**Figure 11.** SW voltammograms of the Cu(II)-PAR complex (—) and PAR (- -) obtained in 0.1 M $KNO_3$ medium, *v* = 200 mV/s.

Reduction peaks of the Cu(II)-PAR complex and PAR were observed at potentials of -0.288 V and -0.609 V, respectively, obtained by adding 100-3500 µl $10^{-4}$ M Cu(II) solution to 800 µl $10^{-4}$ M PAR, as shown in Fig. 11.

A possible analytical feature is noticed when the peak height of the dye gradually decreases as the concentration of metal ions increases, as seen in SWV when the concentration of the dye is fixed at $7.41x10^{-6}$ M (Figs. 12, 13). The peak due to the azo dye disappears when the molar ratio of copper to azo dye reaches approximately 1:2, as shown in Figs. 11 and 12.

As given in Fig. 14, the cathodic peak potentials of the complex and PAR remain approximately constant with increasing concentration of Cu(II).

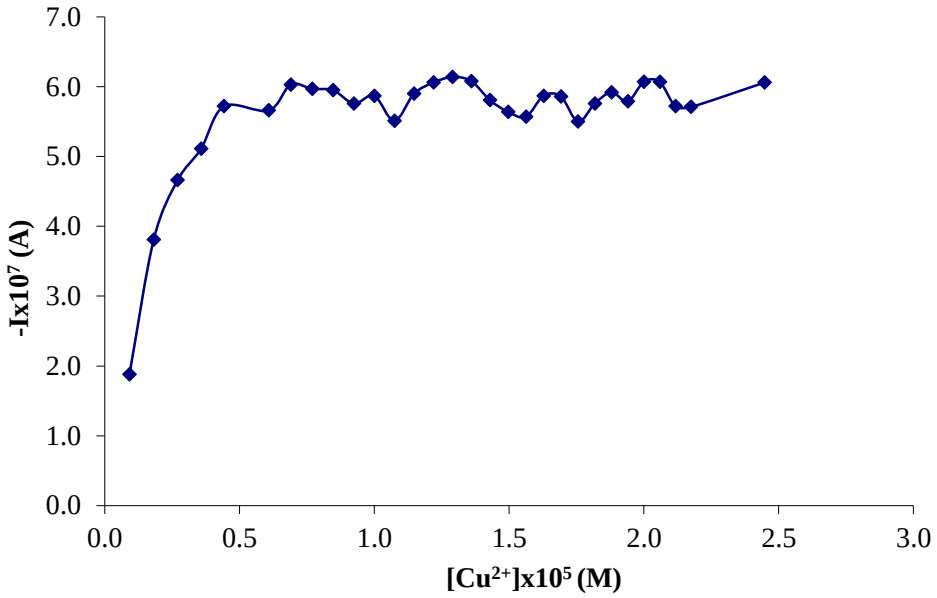


**Figure 12.** The variation in the complex reduction peak current versus added Cu(II) concentration in 0.1 M $KNO_3$ medium.

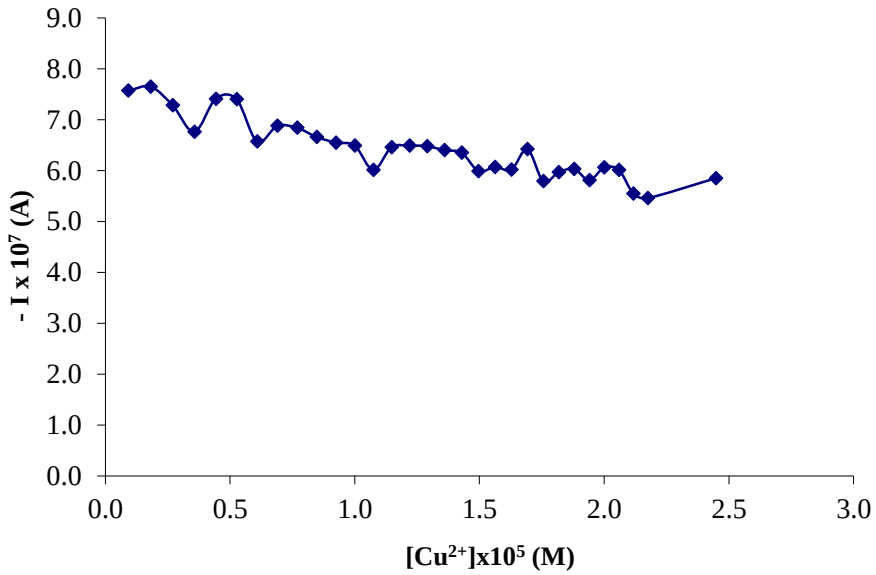


**Figure 13.** The variation in the ligand reduction peak current versus added Cu(II) concentration in 0.1 M $KNO_3$ medium.

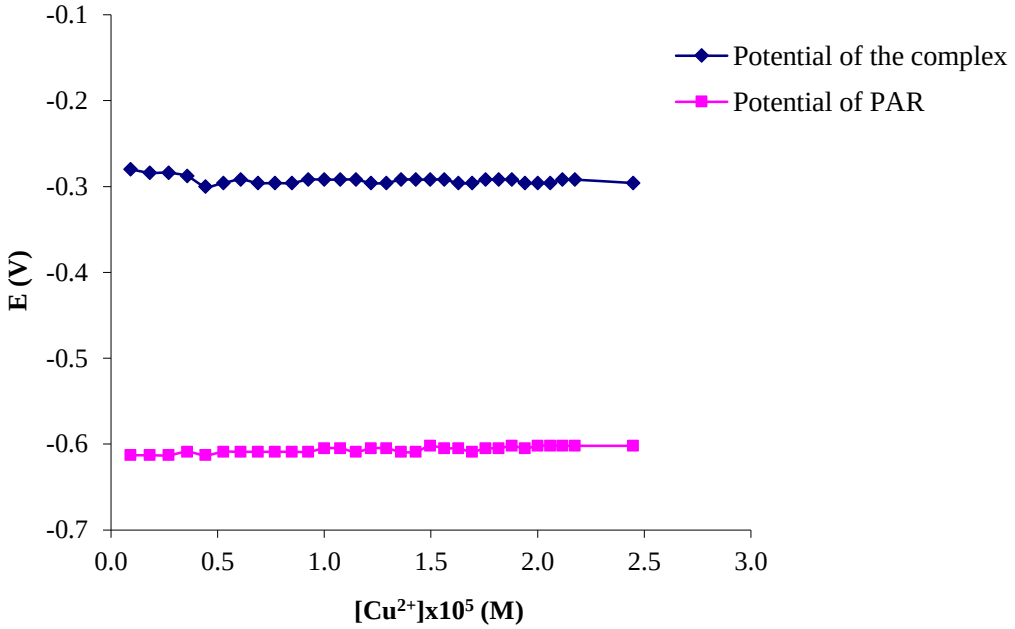


**Figure 14.** The variation in the complex and ligand reduction peak potentials versus added Cu(II) concentration in 0.1 M $KNO_3$ medium.

As another approach, 700 µl $10^{-4}$ M Cu(II) solution was added to 10 ml 0.1 M $KNO_3$ solution in the voltammetric cell. Then, 100-3000 µl $10^{-4}$ M PAR was added to 700 µl $10^{-4}$ M Cu(II), and SW voltammograms were recorded (Fig. 15). The peak potentials of Cu(II), Cu(II)-PAR complex and ligand were determined to be 0.0293 V, -0.312 V and -0.605 V, respectively.

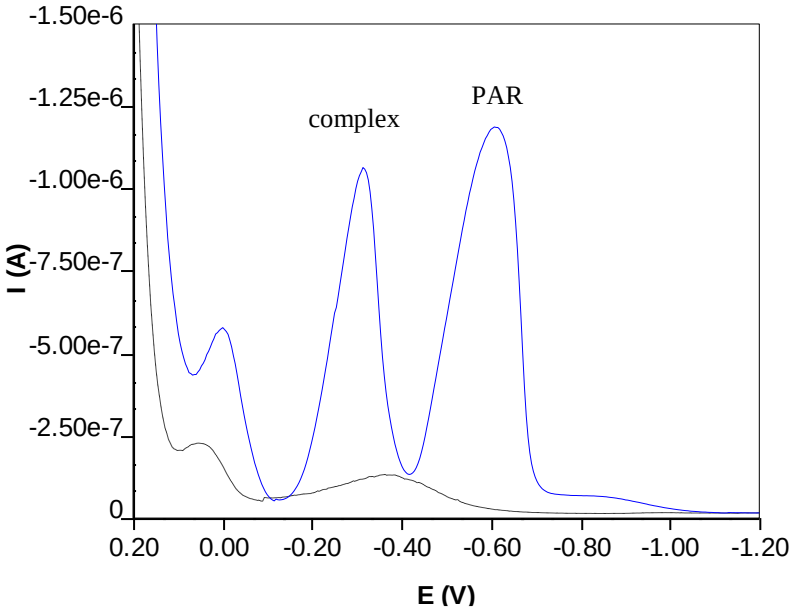


**Figure 15.** SW voltammograms of the Cu(II)-PAR complex (—) and copper(II) (- -) obtained in 0.1 M $KNO_3$ medium, $v$ = 200 mV/s.

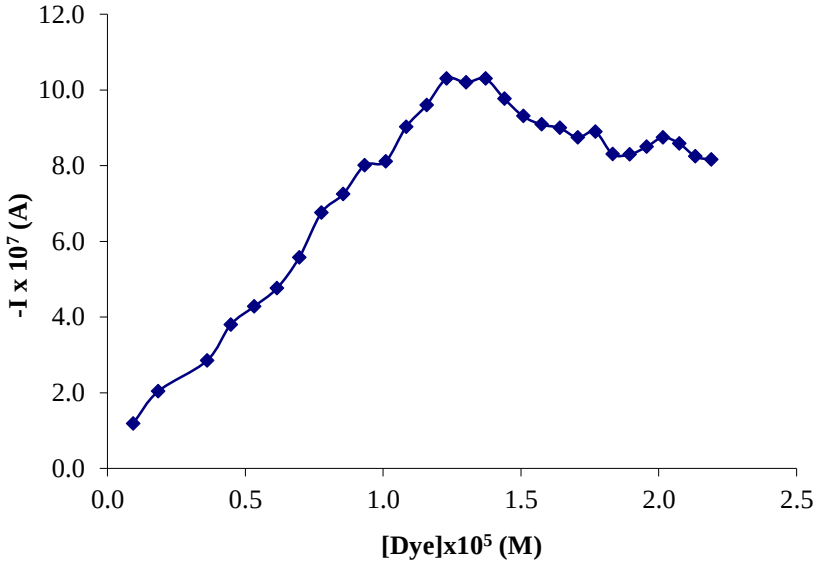


**Figure 16.** The variation in the complex reduction peak current versus added PAR concentration in 0.1 M $KNO_3$ medium.

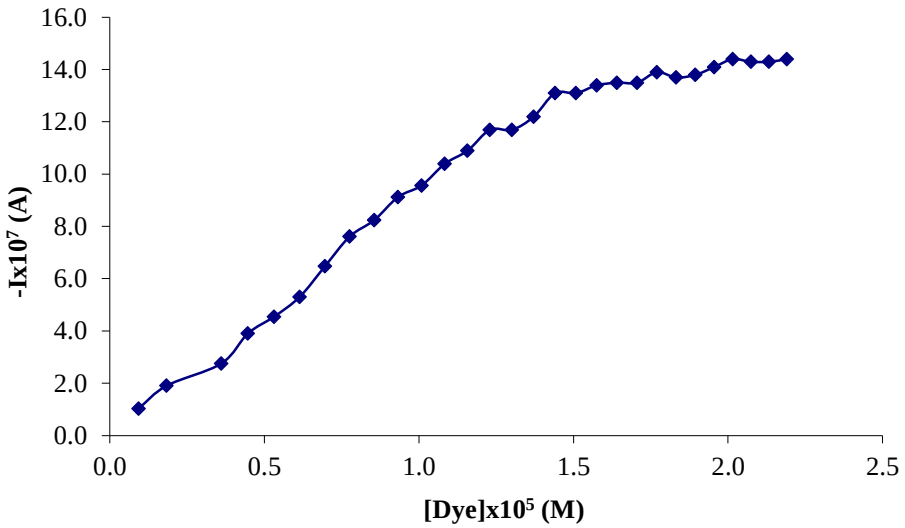


**Figure 17.** The variation in the ligand reduction peak current versus added PAR concentration in 0.1 M $KNO_3$ medium.

By adding 100-3000 µl $10^{-4}$ M PAR to 700 µl $10^{-4}$ M Cu(II), the complex reduction peak decreased with increasing ligand concentration from the point where the metal:ligand ratio was 1:2, as shown in Fig. 16. The reduction peak of the ligand was observed to increase with increasing ligand concentration, as shown in Fig. 17, and the reduction peak potentials of the complex and PAR shifted to more negative potentials with increasing ligand concentration, as shown in Fig. 18.

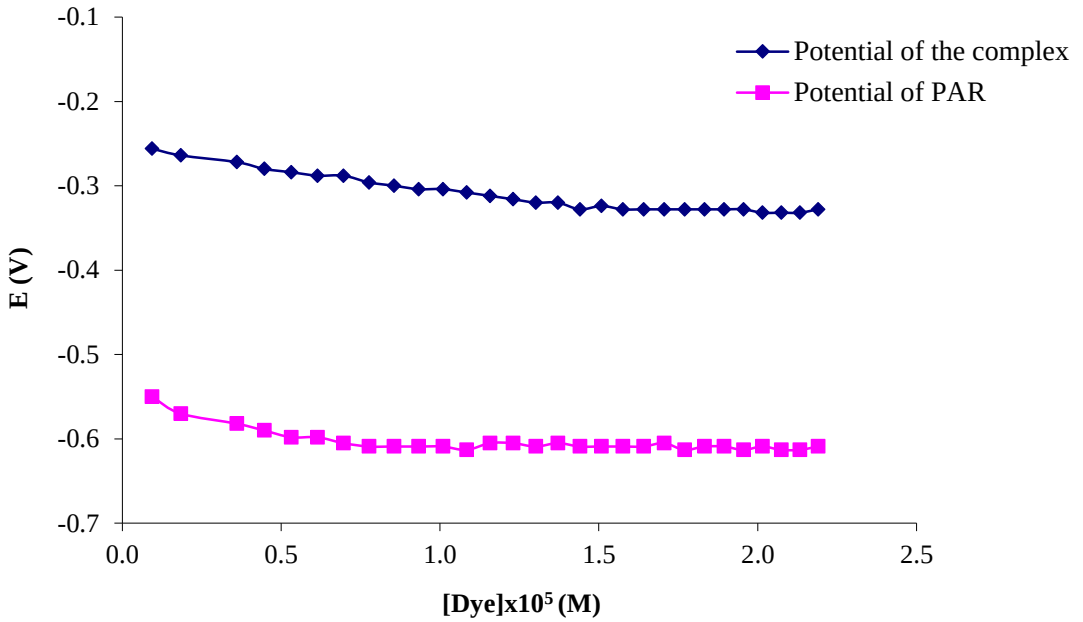


**Figure 18.** The variation in the complex and ligand reduction peak potentials versus added PAR concentration in 0.1 M $KNO_3$ medium.

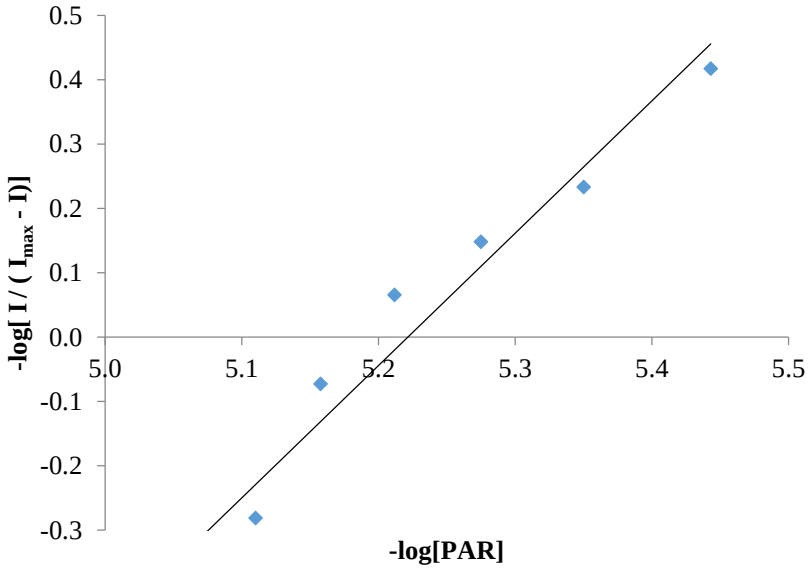


**Figure 19.** The graph of –log[ I / ($I_{max}$ – I)] versus –log[PAR] in 0.1 M $KNO_3$ medium at a HMDE.

To determine the formation constant and metal:ligand molar ratio of the Cu(II)-PAR complex, the following equation was used [5,40,41].

$$Log[ I / (I_{max} – I)] = n \log[PAR] + \log\beta \quad (1)$$

In this equation, I is the peak current of the Cu(II)-PAR complex, $I_{max}$ is the maximum peak current when all the copper ions form the complex and [PAR] is the concentration of PAR. The plot of -log[ I / ($I_{max}$ – I)] versus -log[PAR] is linear. The slope of the graph and intercept give n and –logβ, respectively (Fig. 19). The formation constant of the complex (β) was calculated from the intercept (logβ) of the equation as $5.42x10^{10}$, and the molar ratio of the ligand to metal (n) was determined to be 2.06 from the slope of the equation ($r^2 = 0.96$). The proposed structure of the $Cu(PAR)_2$ complex is given in Scheme 3. Copper azo complexes have been encountered in different forms depending on the solution medium and pH. Especially the formation constants and complex ratios of the complexes of ortho hydroxy azo dyestuffs are more common 1:2. In this study, similar results were found with copper azo dye complexes in spectroscopic, polarographic and voltammetric studies [5, 40-49].

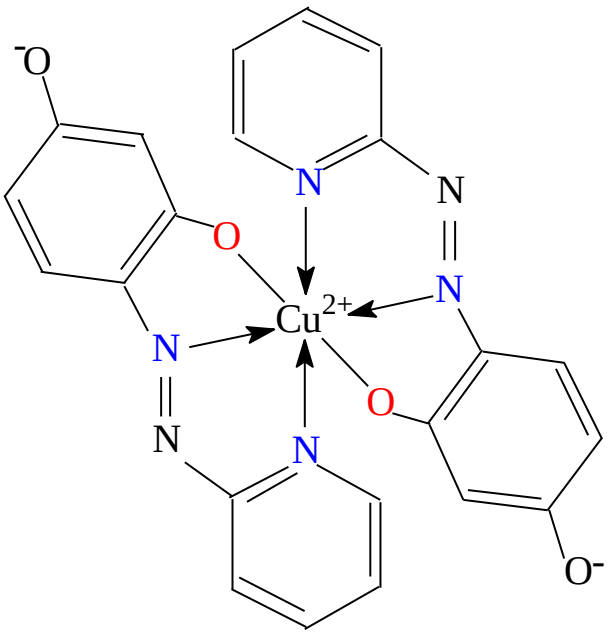


**Scheme 3.** The structure of the $Cu(PAR)_2$ complex.

## 4. CONCLUSIONS

The polarographic and voltammetric behavior of PAR at a SMDE and HMDE has been investigated in BR buffer media by employing SWV, DPP, DCP and CV techniques. The reduction of PAR gives irreversible electrode reaction mechanism behavior in strongly basic media and reversible behavior at pH < 11. Electrode reaction mechanism of PAR has been proposed from the electrochemical data (Scheme 2). At the same time, the molar ratio of the metal to ligand in the Cu(II)-PAR complex was determined by SWV by adding ligand solution to the metal and metal solution to the ligand in 0.1

M $KNO_3$ supporting electrolyte. From these data, the metal:ligand molar ratio of the Cu(II)-PAR complex was found to be 1:2. The stability constant of $Cu(PAR)_2$ was calculated to be $5.42x10^{10}$.

ACKNOWLEDGMENTS
The author is grateful to the Scientific Research Coordination Unit of Sinop University (Project no. FEF-1901-12-01) for financial support of this work.

**References**

1. D. A. Johnson, T. M. Florence, *Anal. Chim. Acta*, 53 (1971) 73.
2. A. S. Amin, A. S. AL-Attas, *J. Saudi Chem. Soc.*, 16 (2012) 451.
3. H. J. Mohammed, A. A. Syhood, *J. Anal. Pharmaceut. Res.*, 7 (2018) 504.
4. M. Ucar, A. O. Solak, N. Menek, *Anal. Sci.*, 18 (2002) 997.
5. Y. Karaman, N. Menek, F. Arslan Bicer, H. Olmez, *Int. J. Electrochem. Sci.*, 10 (2015) 3106.
6. N. A. Meredith, J. Volckens and C. S. Henry, *Anal. Methods*, 9 (2017) 534.
7. N. Menek, *Anal. Lett.*, 31 (1998) 275.
8. S. Menati, A. Azadbakht, R. Azadbakht, A. Taeb, A. Kakanejadifard, *Dyes Pigments*, 98 (2013) 499.
9. L. Dubenska, H. Levytska, N. Poperechna, *Talanta*, 54 (2001) 221.
10. S. Pysarevska, L. Dubenska, N. Shajnoga, H. Levytska, *Chem. Met. Alloys*, 2 (2009) 194.
11. S. Patai, *The Chemistry of the Hydrazo, Azo and Azoxy Groups*, John Wiley&Sons, (1975) London.
12. S. Pysarevska, L. Dubenska, I. Spanik, J. Kovalyshyn and S. Tvorynska, *J. Chem.*, 2013 (2013) 1.
13. A. G. Fogg, A. Rahim, H. M. Yusoff, R. Ahmad, *Talanta*, 44 (1997) 125.
14. A. G. Fogg, R. Ismail, R. Ahmad, S. L. Williams and M. V. B. Zanoni, *Microchem. J.*, 57 (1997) 110.
15. S. V. Smirnova, T. O. Samarina, D. V. Ilin and I. V. Pletnev, *Mosc. Univ. Chem. Bull.*, 70 (2015) 229.
16. A. A. Ramadan, H. Mandil and A. A. Kamel, *Asian J. Chem.*, 21 (2009) 7367.
17. B. Nigovic, B. Simunic, S. Hocevar, *Electrochim. Acta*, 54 (2009) 5678.
18. N. Menek, S. Basaran, Y. Karaman, S. Topcu, *Int. J. Electrochem. Sci.,* 8 (2013) 6399.
19. Y. Karaman, *Dyes Pigments,* 106 (2014) 39.
20. A. Radi, M. R. Mostafa, T. A. Hegazy, R. M. Elshafey, *J. Anal. Chem.,* 67 (2012) 890.
21. A. E. Radi, H. M. Nassef, A. El-Basiony, *Dyes Pigments,* 99 (2013) 924.
22. R. Jain, N. Sharma, K. Radhapyari, *J. Appl. Electrochem,.* 39 (2009) 577.
23. Y. Karaman, N. Menek, *J. Electrochem. Soc.,* 159 (2012) H805.
24. P. Zuman and C. L. Perin, *Organic Polarography*, John Wiley & Sons, (1965) New York.
25. L. Meites, *Polarographic Techniques*, John Wiley & Sons, (1965) New York.
26. A. J. Bard and L. R. Faulkner, *Electrochemical Methods*, JohnWiley & Sons, (1980) New York.
27. M. Abdallah, M. M. Alfakeer, N. F. Hasan, A. M. Alharbi and E. M. Mabrouk, *Orient. J. Chem.,* 35 (2019) 98.
28. J. Barek, D. Civisova, A. Ghosh, and J. Zima, *Collect. Czech. Chem. Commun.*, 55 (1990) 379.
29. A. G. Fogg, M. V. B. Zanoni, A. Rahim, H. M. Yusoff, R. Ahmad, J. Barek, and J. Zima, *Anal. Chim. Acta*, 362 (1998) 235.
30. M. P. Char, E. Niranjana, B. E. Kumara Swamy, B.S. Sherigara, V. Pai, *Int. J. Electrochem. Sci.,* 3 (2008) 588.

31. S. El Aggadi, N. Loudiyi, A. Chadil, O. Cherkaoui and A. El Hourch, *Mediterr. J. Chem.,* 9 (2020) 82.
32. U. Chandra, O. Gilbert, B. E. Kumara Swamy, Y. D. Bodke, B. S. Sherigara, *Int. J. Electrochem. Sci.,* 3 (2008) 1044.
33. S. Momeni & D. Nematollahi, *Sci. Rep.,* 7 (2017) 41963.
34. M. B. Leitner, R. Ruhmann and J. Springer, *Polym. Advan. Technol.,* 7 (1996) 437.
35. N. Menek, O. Çakır, H. Kocaokutgen, *Mikrochim. Acta,* 122 (1996) 203.
36. D. Dion, E. Laviron, *Electrochim. Acta,* 43 (1998) 2061.
37. M. V. B. Zanoni, P. A. Carneiro, M. Furlan, E. S. Duarte, C. C. I. Guaratini, A. G. Fogg, *Anal. Chim. Acta,* 385 (1999) 385.
38. B. Nigovic, S. Komorsky-Lovric, B. Simunic, *Electroanalysis*, 17 (2005) 839.
39. W. Lai-Hao and H. Shu-Juan, *J. Autom. Methods Manag.,* 2011 (2011) 896978.
40. E. Bicer and C. Arat, *J. Chil. Chem. Soc.,* 53 (2008) 1734.
41. N. Menek, S. Topcu and M. Ucar, *Anal. Lett.,* 34 (2001) 1733.
42. E. Ispir, M. Ikiz, A. Inan, A. B. Sunbul, S. E. Tayhan, S. Bilgin, M. Kose, M. Elmastas, *J. Mol. Struct.* 1182 (2019) 63.
43. I. A. Salem, M. H. Shaltout, A. B. Zaki, *Spectrochim. Acta A Mol. Biomol. Spectrosc.* 227 (2020) 117618.
44. A. M. Khedr, H. El-Ghamry, M. A. Kassema, F. A. Saad, N. El-Guesmi, *Inorg. Chem. Commun.,*108 (2019) 107496.
45. E. Raafid, M. A. Al-Da'amy, and S. H. Kadhim, *Indones. J. Chem.,* 20 (2020) 1080.
46. S. Asiri, M. A. Kassem, M. A. Eltaher, K. M. Saad, *Int. J. Electrochem. Sci.,* 15 (2020) 6508.
47. A. Kochem, A. Carrillo, C. Philouze, M. van Gastel, A. du M. d'Hardemare, and F. Thomas, *Eur. J. Inorg. Chem.,* 2014 (2014) 4263.
48. F. Kunitake, J-Y. Kim, S. Yagi, S. Yamzaki, T. Haraguchi and T. Akitsu, *Symmetry,* 11 (2019) 666.
49. N. Venugopal, · G. Krishnamurthy, · H. S. B. Naik, · J. D. Manohara, *J. Inorg. Organomet. Polym. Mater.,* 30 (2020) 2608.